Journal of Materials Chemistry C

Accepted Manuscript

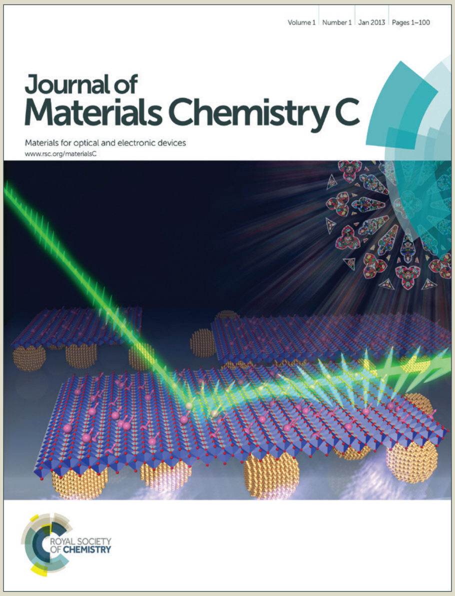

ROYAL SOCIETY OF CHEMISTRY

www.rsc.org/materialsC

Cite this: DOI: 10.1039/c0xx00000x

www.rsc.org/xxxxxx

ARTICLE TYPE

Fabrication of homogenous three dimensionally ordered conducting polymer-polystyrene opal structures in microfluidic channels

Brian Gorey[a], *Malcolm R. Smyth*[a], *Blánaid White*[a], *Aoife Morrin*[*a]

[a]National Centre for Sensor Research, School of Chemical Sciences, Dublin City University, Dublin 9, Ireland
*aoife.morrin@dcu.ie

Received (in XXX, XXX) Xth XXXXXXXXX 20XX, Accepted Xth XXXXXXXXX 20XX
DOI: 10.1039/b000000x.

Abstract

A chemical polymerisation method for fabricating an electrochemically addressable, three dimensionally (3-D) ordered homogenous polyaniline (PANI)-based opal structure in a microfluidic channel is described. Electrochemical polymerisation was also explored as a route to creating opal structures of PANI. Interestingly, electrochemical growth resulted in an inhomogeneous gradient-type morphology throughout the depth of the template leading to non-uniform 3-D PANI structures. Using the chemical polymerisation approach, a thin coating of PANI could be deposited homogeneously to the PS sphere surfaces. This coating was electrochemically accessible subsequent to an electrochemical polymerisation step electrically connecting the opal structure to an integrated gold electrode within the microchannel. Electrochemical characterisation of the resultant ordered PANI-PS material in-channel, demonstrated the synthesis of a well behaved, stable PANI coating throughout the PS CC which behaves as a thin film with fast electron transfer.

1 Introduction

Intrinsically conducting polymers (ICPs) are organic polymeric materials which display electrical, magnetic and optical properties normally associated with metals.[1-4] Some examples of common ICPs include polypyrrole (PPY) polythiophene (PT) and polyaniline (PANI). The conjugated backbone of such polymers affords them high conductivities. The combination of traditional polymer properties as well as electrically conductive properties[5] makes ICPs applicable in many areas of research. Applications include sensors,[3, 6] energy storage,[7-9] drug delivery systems (DDS)[10-13] and separations.[14-16]

A drawback of current ICP fabrication methods is the relatively poor reproducibility of bulk ICPs. A move to nano- or micro-structured ICP materials has shown benefits with the properties of ICPs dramatically improved or even changed,[17, 18] with quicker response times noted in sensing in the case of PANI[19] as well as reproducibility in ICP structure. Methods available to template fall into two main categories; soft-templating[20-23] and hard-templating. Hard templating requires a physical template which directs the growth of ICP's during polymerisation. Common templates, which may remain in place or be removed subsequent to ICP polymerisation, include silica and PS spheres.[24] These templates have been widely used for the fabrication of inverse opals of ICP materials.[25-28] These three-dimensionally ordered macro-porous (3-DOM) ICP materials offer improved performance over bulk and even other nanostructured materials due to the interconnected pores, large surface areas and porosities. They can be fabricated chemically and electrochemically. Distinct advantages in the application of these materials are emerging in the literature. For example, Ge *et al.* fabricated PANI 3-DOM materials electrochemically on planar indium tin oxide (ITO) through a PS sphere template deposited via a vertical drying method. It was demonstrated that ion diffusion reversibility and ion storage were greatly improved over bulk material due to the interconnected porous structure, which benefits from the fast penetration of ions.[28] Tian *et al.* also electrochemically polymerised aniline through a PS CC. The incorporated dopants were shown to significantly effect the structure and the mechanical stabilities of the opaline films. Also, the rate of polymerisation was studied. It was shown that once polymerisation through the internal structure of the template had taken place, the rate of polymerisation increased dramatically. This was ascribed to a rapid increase of the electrochemical reaction area once the growth front of the deposited material reached the template/bulk solution interface.[29] Chemical polymerisation can also be used to achieve 3-DOM PANI structures. Yang & Liau fabricated inverse opals of PANI by immersing PS CC films on glass slides in aqueous solutions of dodecylbenzene sulfonic acid (DBSA), followed by the addition of aniline in HCl and APS. High quality, high surface area PANI with pore interconnectivity was achieved.[30] Chemical polymerisation was also used to form another type of 3-D structure, PANI-infiltrated TiO_2 inverse opal photonic crystals.[31] In this instance, aniline was chemically polymerised through TiO_2 inverse opals fabricated through PS templating. These structures were shown to be optically sensitive to pH. Hard templating of other conducting polymers has also been carried out. For example, Santos *et al.* described the fabrication of 2-D ordered PPY via electrochemical polymerisation again on planar substrates.[32] The 2-D PS template was prepared via the vertical deposition method using PS spheres bearing hydrophilic shells. By controlling the charge passed during the polymerisation, the growth of PPY could be controlled leading to control over the depth and corresponding diameters of the resulting pores.[32] Several other recent examples of 3D ordered polymerisations of ICPs are present in the literature.[28, 33-35] While the majority of these templated ICP structures are fabricated on planar substrates, it is critical that these structures can also be fabricated in a range of other formats in order to truly realise their full potential. The microfluidic channel is one such format that has a potential use for flow-through electrochemical sensing and separations. It can be envisaged that 3-DOM ICP structures could have numerous applications in such a format where the flow-through nature and high surface area of these structures can be exploited under flowing conditions. Achieving the desired homogeneous 3-D structure of the ICP within a microfluidic channel is required in the first instance and is demonstrated in this research.

It is generally assumed in the literature that if the 3-D CC template structure is uniform throughout, the resulting template directed ICP will also possess this structural homogeneity. Indeed, the advantages attributed to 3-DOM are often dependent upon such inverse opal homogeneity.[36, 37] However, template directed polymerisation methods, such as electrochemical polymerisation, do not necessarily result in this assumed homogeneity. Here, the potential for structural inhomogeneity as a result of electropolymerisation through a hard template is demonstrated. An alternate polymerisation strategy to overcome these inhomogeneities has been developed where a chemical polymerisation of 3-D PANI through a CC PS template, fabricated through a simple one step capillary force packing method results in a 3-D ordered PANI structure. The electrochemical characterisation of these structures shows these structures to exhibit rapid electrochemical switching, showing their potential use for advanced lab-on-a-chip electrochemical applications.

2 Experimental

2.1 Materials

1 µm PS spheres were purchased from Duke Scientific (Palo Alto, California, USA). Deionised (DI) water was purified using a MilliQ system to a specific resistance of greater than 18.2 MΩ-cm. A silver/silver chloride reference electrode (CHI111) was purchased from CH Instruments, Inc. (USA). A platinum mesh from Sigma Aldrich (Dublin) was used as the auxiliary electrode (298107). Polydimethylsiloxane (PDMS) (101697) (Dow Corning 184 silicone elastomer), was purchased from Farnell (Ireland). All other chemicals were purchased from Sigma-Aldrich (Dublin) and were of analytical grade. All reagents were used as purchased with the exception of aniline which was distilled prior to use.

2.2 Instrumentation

Scanning electron micrographs (SEM) were obtained using a Hitachi S3400N scanning electron microscope (Hitachi, UK) at an acceleration voltage of 20 kV, probe current of 35 µA and working distance of 10 mm. All samples were gold and chromium-sputtered using a 750T sputter coater, Quorum Technologies (UK). A CHI600c electrochemical analyser (CH Instruments Inc., USA) was used for all electrochemical experiments. A CMA microinjection system (Microdialysis, Sweden) was used for all flow-through experiments. All oxygen plasma treatment was performed using a Harrick plasma cleaner PDC-001 expanded model.

2.3 Methods

2.3.1 PDMS chip fabrication incorporating an electrochemical cell

Silicone elastomer and curing agent were mixed in a 1:10 w/v ratio, degassed for 45-60 min under vacuum, and poured onto a silicone mould that was prepared using photolithography with resulting channel depth of 0.110 mm or 0.220 mm,as specified, and cured at 100°C on a hotplate for 45 min. PDMS chips were then cut to correct size, 45 mm x 20 mm, after curing. PDMS and glass final T-channel dimensions were 0.110 mm x 0.110 mm x 40 mm or 0.220 mm x 0.220 mm x 40 mm. A well was punctured into the PDMS chips at the inlet to enlarge it to 3 cm approx. in diameter. The reference and auxiliary electrodes were housed in the well during electrochemical experiments as detailed previously.[38] For incorporation of a WE, PDMS chips were masked to isolate the microfluidic channel using duct tape, and then gold sputtered for 2.5 min at 50 mA (0.110 mm x 40 mm). Alternatively, gold was sputtered to a glass slide to form the WE using an mask corresponding to same dimensions. Sealing of chips was achieved through oxygen plasma treatment of the surface of the PDMS chip and a glass slide for 5 min before sealing together and applying pressure for 20-30 s. were

2.3.2 PS colloidal crystal formation

PS CCs were fabricated within the microchannels as detailed previously using capillary force action.[39] A 1% w/v PS suspension of 1 µm spheres was used to form all CCs. The length of the CC along the channel was controlled by localising the oxygen plasma treatment to particular length of channel e.g. 5 mm, using a mask.

2.3.3 Electrochemical polymerisation of aniline through CC template

A microchip containing a PS CC was immersed in a solution of 9.8 mL HCl (1 M) containing 200 µL of distilled aniline (2.2 x 10^{-2} M) for 10 min before polymerisation to allow the aniline solution to infiltrate the PS sphere template. A potential of +0.9 V vs. Ag/AgCl was applied for 210 s, as optimised previously.[39] After polymerisation, the PANI was allowed to air dry for 20 min before immersing the chip in toluene to dissolve out the PS template.

2.3.4 Preparation of aniline-coated PS spheres

81.6 µL of aniline (2.2 x 10^{-3} M) was added to 0.4 g of 1 µm PS sphere in 40 mL of DI water under constant stirring for 30 min. The aniline-coated PS spheres were then centrifuged down at 5000 rpm for 7 min to remove excess aniline in solution. The spheres were then re-dispersed in 40 mL DI water resulting in a 1% w/v aniline-coated PS sphere suspension.

2.3.5 Chemical polymerisation of aniline-coated PS CC

Aniline-coated PS was used to form CCs within the PDMS microchannels according to Section 2.3.2. The microchips were then immersed in a solution of APS (7.8 x 10^{-3} M) in 10 mL of HCl (1 M) at room temperature and left standing for 8 hr. After polymerisation, the PANI was washed in D.I. water for 20 s and subsequently allowed to air dry for 20 min. The microchip was then sealed, using oxygen plasma treatment for 5 min to a glass slide with an integrated gold WE. A 10 segment voltammetric cycle between -0.3 and +1.1 V vs. Ag/AgCl was performed at a scan rate of 0.1 V s^{-1} to induce a consistent electrical bridge between the PANI-coated CC and the underlying WE.

3 Results and discussion

3.1 Electrochemical polymerisation of PANI through CC template

CCs were first formed in the microchannels according to Methods Section 2.3.2. The capillary force packing used to obtain these crystals resulted in crystals with depths equivalent to the depth of the microchannel itself. Thus the resulting CC depth was 0.110 mm or 0.220 mm, depending on the depth of channel used. Electrochemical polymerisation of aniline was carried out potentiostatically in unsealed microchannels through CC templates for 210 s.[39] This was expected to result in a homogeneous, opal template directed 3-D PANI structure. However, when internal sections of the resulting PANI structure were imaged by SEM (Fig. 1), subsequent to the removal of the template, it could be seen that the morphology of the PANI varied over its depth. In images of the upper layers of the structure, furthest from the integrated gold WE (sputtered along the base of the microchannel), the PANI monolith showed some areas comprising the desired flow-through pores (Fig. 1A). However, the structure appeared fragile and contained defects, as highlighted within the green circle in Fig. 1A. Moving down the depth of the channel towards mid-way, the density of the PANI morphology increased (Fig. 1B). The desired flow-through pores arising from the template directed growth were present. An example of this is shown inside the green circle in Fig. 1B. Some defects were also evident due to the stripping of upper layers to view the internal structure of the PANI monolith. Finally along the lower areas of the channel, closest to the WE, PANI had the densest morphology (Fig. 1C). The desired flow-through pores were sealed resulting in loss of interconnectivity through the PANI structure. This is highlighted within the green circle in Fig. 1C. The reason for this observed morphology gradient can be explained by detailing the process for electropolymerisation. At the surface of an electrode, this process consists of three steps; 1) radical formation 2) coupling of radicals and 3) further oxidation resulting in chain propagation.[40] As propagation continues, increasing amounts of polymer are formed as a function of time.[41, 42] This results in immediate polymer growth closest to the WE, as polymerisation is on-going in this vicinity for the full duration of the experiment (210 s in this instance). As PANI propagation continues over time, polymer formation continues close to the WE as well as extending out to the growth front which becomes increasingly distant from the WE over time. This growth is facilitated by the nucleation sites at the growth front of the PANI. As propagation can only occur on the outer surface at these latter times, the duration of polymerisation in these areas is shorter than the timescale of the experiment (210 s), ultimately resulting in less polymer growth in these areas in comparison to that grown at the WE surface. This gradient nature of the polymerisation is reflected in the changing morphology noted through the depth of the microchannel (0.110 mm) as seen in Fig. 1.

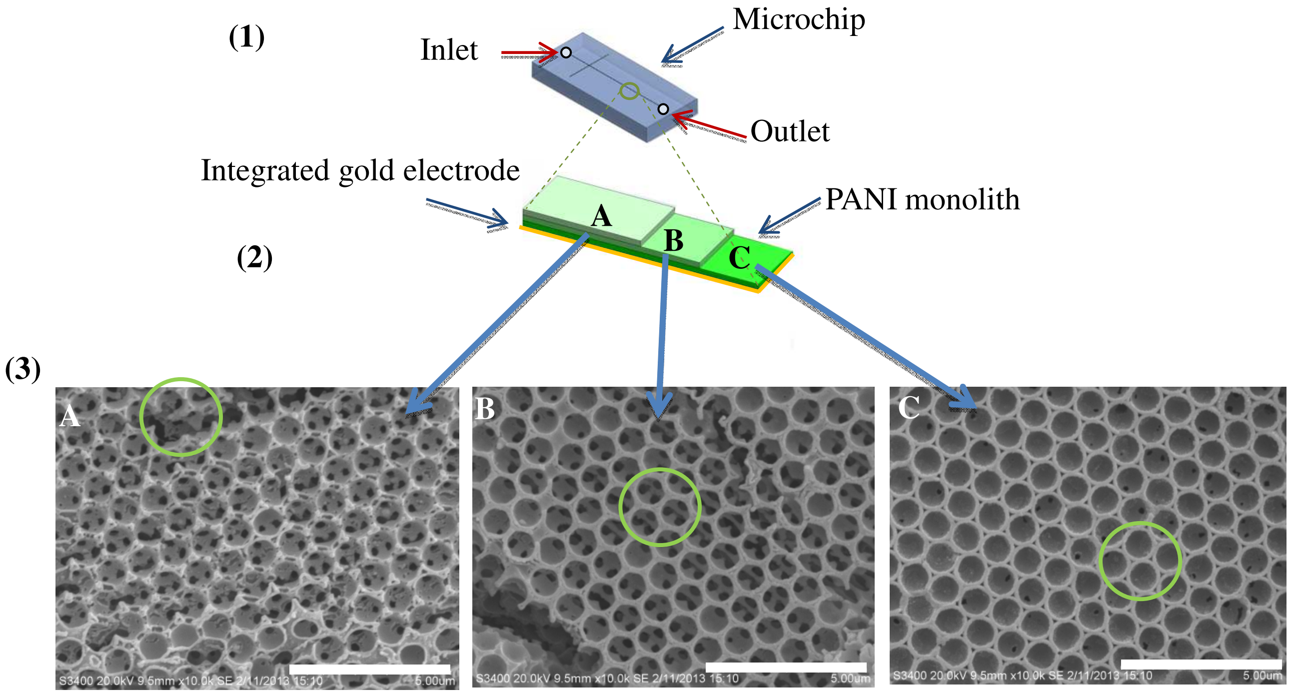

Fig. 1 Schematic of (1) µchip containing a microchannel (0.110 mm) housing (2) an electrochemically grown monolith where areas of the monolith are defined (3) SEM images of PANI monolith structures after removal of PS template. A) Upper layer of 3-DOM inverse opal furthest from the WE. B) Middle layer of 3-DOM inverse opal. C) Lower layer of 3-DOM inverse opal, closest to WE. Mag: 10.0k; scale bar: 5.00 µm.

3.3 Chemical polymerisation of PANI through CC template

An attempt to overcome the density gradient issue observed for electrochemical polymerisation was undertaken. To induce polymerisation initiation sites homogenously dispersed throughout the PS template, aniline-coated PS spheres were prepared. As detailed in the Methods Section 2.3.4, 1 µm PS spheres were exposed to aniline in an aqueous medium. Hydrophobic-hydrophobic interactions and π-π interactions between the aromatic backbone of the PS and benzene ring of the aniline monomer facilitated adsorption of aniline to the PS spheres. A schematic showing the adsorption of aniline to a PS sphere and its subsequent polymerisation is detailed in Scheme 1. After modification, the aniline-coated PS spheres were packed uniformly in channel by capillary force packing according to Methods Section 2.3.2. The aniline coating was then chemically polymerised in chip in both unsealed and sealed channel formats.

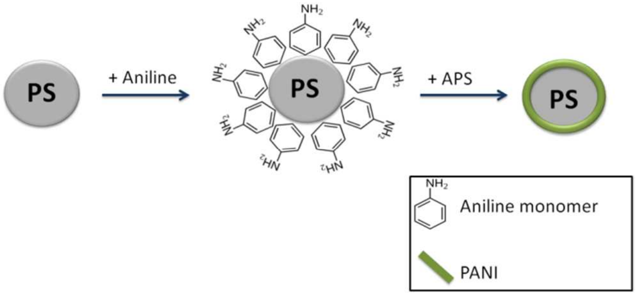

Scheme 1 Schematic of PS sphere coating with aniline and subsequent surface confined polymerisation of PANI on individual PS spheres.

After chemical polymerisation of the aniline, a thin coating of PANI was observed through the CC.[43] Due to the fragility of the PANI coatings, the CC template was kept in place to act as a supporting scaffold resulting in a 3-D PANI-PS structured opal. In this PANI-coated PS sphere composite structure, flow-through was achieved through the interstitial and channel voids (as highlighted by green and blue circles in Fig. 2) that were present between PS spheres in the face centred cubic (fcc) structure.

Using this chemical polymerisation approach, a homogeneous PANI coverage throughout the full depth of the microchannel was achieved, Fig.2A-C. SEM images were taken of internal upper, middle and lower layers of the PANI-PS opal structure corresponding to the approximate areas previously noted during electrochemical polymerisation, as seen in Fig. 1A-C. Here, PANI which was chemically polymerised in a sealed microchannel under flow conditions, exhibited equivalent morphologies in each area. A thin layer of PANI present within the channel voids (circled in blue) and interstitial voids (circled in green) of the CC structure was observed as presented in Fig. 2A. The flow profile of oxidant/HCl solution through the fcc CC structures dictates that polymerisation can only occur in the voids present between PS spheres. Where PS spheres contact, no polymerisation can occur as flow cannot reach these areas. Fig. 2D-F show the inverse images obtained through contrast conversion of images A-C, further illustrating the voids where chemical polymerisation occurs. Thus the inhomogeneity during electrochemical polymerisation was shown to have been successfully overcome with this approach. Homogeneous PANI coverage was achieved here throughout the opal structure (0.220 mm depth) within a microchannel.

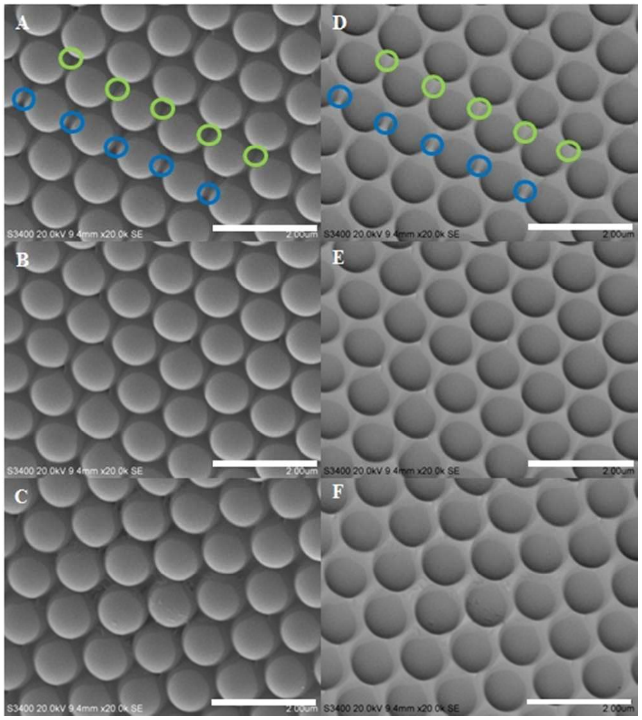

Fig. 2 SEM images of PANI-coated CC structures illustrating representative internal layers as follows: A) upper layer B) middle layer and C) lower layer of PANI-PS CC (microchannel depth 0.220 mm). Thin layers of PANI present within the channel voids are circled in blue, interstitial voids are circled in green. Images D-F show the contrast converted images of A-C resulting in a higher emphasis visually, on the interstitial and channel voids between each sphere of the original images. Mag: 20.0 k; scale bar: 2.00 μm.

3.5 Investigation of electrochemical behaviour of PANI-PS opals

After chemical polymerisation of the aniline-coated PS CC, the electrochemical behaviour of the system was investigated. It was found that the electrochemistry of the PANI-coated CC could only be accessed after electropolymerising PANI to the microchannel integrated gold WE. This induced a stable electrical connection between the WE and the soft, thin PANI coating on the CC.

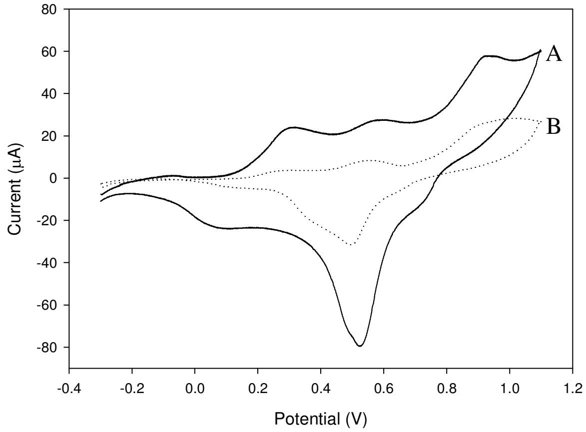

Fig. 3 A) Cyclic voltammetry of PANI-coated PS CC in a sealed microchannel where an electropolymerisation of aniline is used to electrically connect the PANI structure to the WE. A control is also shown B) of a bare PS CC upon electrochemical polymerisation of aniline to mimic the same electrical connection.

Fig. 3A shows the electrochemistry observed in the microchannel in the presence of the PANI-PS opal after electrochemical synthesis of the PANI-based electrical connection. Typical PANI electrochemistry is obtained that is dominated by the chemically polymerised PANI-PS opal structure. To verify that this electrochemistry was primarily attributed to the chemically deposited PANI, PANI was electrochemically grown to induce the same electrochemical connection from the integrated WE to a bare PS opal as a control (Fig. 3B). It can be seen in the control experiment that, although PANI electrochemistry is evident, currents were significantly lower than those resulting from the PANI-coated PS opal structure, demonstrating that the electrochemistry of the chemically polymerised PANI-PS opal structure could be successfully accessed by this approach.

To further characterise the 3-D PANI structure, a scan rate study was performed (Fig. 4). The oxidation peaks can be assigned to oxidation of leucoemeraldine (LM) to its radical cation (a), and from LM radical cation to emeraldine (EM) (b). The reduction peaks are assigned to the reduction of EM to its radical cation (c) and finally EM cation to LM (d).[44] Fig. 4 inset is a graph of i_p vs. scan rate^{½}. It shows a high linearity ($R^2 = 0.992$), demonstrating a well behaved, stable PANI coating behaving as a thin film with fast electron transfer.

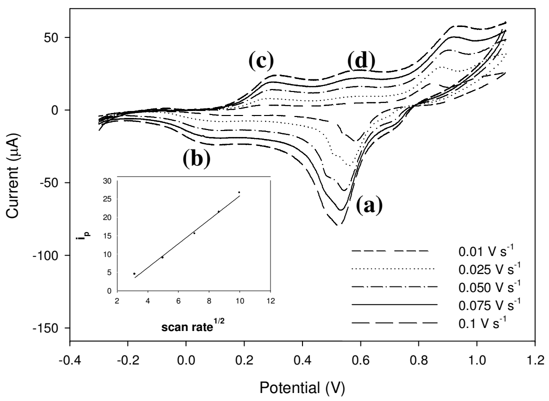

Fig. 4 Scan rate study performed of the PANI-PS opal structure from 0.01 – 0.1 V s^{-1} in HCl (1 M) vs. Ag/AgCl. Inset graph of i_p vs. scan rate^{½} with $R^2 = 0.992$.

4 Conclusion

A novel template directed chemical polymerisation strategy was developed to produce a 3-D ordered PANI-PS opal structure within the confines of a microchannel. Electrochemical polymerisation ensured a consistent connection between the PANI-PS opal structure and the integrated gold WE, ensuring that the PANI opal structure was fully addressable electrochemically. The PANI coating displayed thin film electrochemistry with fast electron transfer. Thus, this approach is a viable route to obtaining homogenous, electrochemically-responsive, ordered, flow-through materials directly within microchannels. It overcomes inhomogenity issues observed here using an alternate electrochemical polymerisation approach. Applications envisaged for these types of structures include controlled release within microchannels, electrochemically-controllable stationary phases and electrochemical sensing microfluidic platforms.

5 Notes and references:

1. S. Bhadra, D. Khastgir, N. K. Singha and J. H. Lee, *Prog. Polym. Sci.*, 2009, **34**, 783-810.
2. S. Bhadra, N. K. Singha and D. Khastgir, *Synth. Met.*, 2006, **156**, 1148-1154.
3. P. S. Sharma, A. Pietrzyk-Le, F. D'Souza and W. Kutner, *Anal. Bioanal. Chem.*, 2012, **402**, 1-28.
4. A. G. MacDiarmid, *Angew. Chem. Int. Ed.*, 2001, **40**, 2581-2590.
5. R. Holze, *Electrochim. Acta*, 2011, **56**, 10479-10492.
6. M. Anu Prathap, B. Thakur, S. N. Sawant and R. Srivastava, *Colloids Surf., B*, 2011, **89**, 108-116.
7. G. Nyström, M. Strømme, M. Sjödin and L. Nyholm, *Electrochim. Acta*, 2012, **70**, 91-97.
8. A. Razaq, L. Nyholm, M. Sjödin, M. Strømme and A. Mihranyan, *Adv. Energy Mater.*, 2011, **2**, 445-454.

9. K. Gurunathan, A. V. Murugan, R. Marimuthu, U. Mulik and D. Amalnerkar, *Mater. Chem. Phys.*, 1999, **61**, 173-191.
10. D. Svirskis, J. Travas-Sejdic, A. Rodgers and S. Garg, *J Control. Release*, 2010, **146**, 6-15.
11. R. T. Richardson, A. K. Wise, B. C. Thompson, B. O. Flynn, P. J. Atkinson, N. J. Fretwell, J. B. Fallon, G. G. Wallace, R. K. Shepherd and G. M. Clark, *Biomaterials*, 2009, **30**, 2614-2624.
12. M. R. Abidian and D. C. Martin, *Adv. Funct. Mater.*, 2009, **19**, 573-585.
13. R. Wadhwa, C. F. Lagenaur and X. T. Cui, *J. Control. Release*, 2006, **110**, 531-541.
14. H. Ge and G. Wallace, *Anal. Chem.*, 1989, **61**, 2391-2394.
15. R. S. Deinhammer, K. Shimazu and M. D. Porter, *Anal. Chem.*, 1991, **63**, 1889-1894.
16. B. J. Yakes, D. W. Keller and M. D. Porter, *J Chromatogr. A*, 2010, **1217**, 4395-4401.
17. Y. Z. Long, M. M. Li, C. Gu, M. Wan, J. L. Duvail, Z. Liu and Z. Fan, *Prog. Polym. Sci.*, 2011, **36**, 1415-1442.
18. A. Thomas, F. Goettmann and M. Antonietti, *Chem. Mater.*, 2008, **20**, 738-755.
19. Z. F. Li, F. D. Blum, M. F. Bertino, C. S. Kim and S. K. Pillalamarri, *Sens. Actuators, B* 2008, **134**, 31-35.
20. J. Huang, S. Virji, B. H. Weiller and R. B. Kaner, *J. Am. Chem. Soc.*, 2003, **125**, 314-315.
21. J. Huang and R. B. Kaner, *J Am. Chem. Soc.*, 2004, **126**, 851-855.
22. B. Bhowmick, D. Mondal, D. Maity, M. Rahaman Mollick, M. Kanti Bain, N. Kumar Bera, D. Rana, S. Chattopadhyay and D. Chattopadhyay, *J. Appl. Polym. Sci.*, 2013, **129**, 3551-3557.
23. D. Pahovnik, E. Žagar, K. Kogej, J. Vohlídal and M. Žigon, *Eur. Polym. J.*, 2013, **49**, 1381-1390.
24. A. Stein, F. Li and N. R. Denny, *Chem. Mater.*, 2007, **20**, 649-666.
25. M. Heim, S. Reculusa, S. Ravaine and A. Kuhn, *Adv. Funct. Mater.*, 2012, **22**, 538-545.
26. L. Zhao, L. Tong, C. Li, Z. Gu and G. Shi, *J. Mater. Chem.*, 2009, **19**, 1653-1658.
27. X. H. Li, L. Dai, Y. Liu, X. J. Chen, W. Yan, L. P. Jiang and J. J. Zhu, *Adv. Funct. Mater.*, 2009, **19**, 3120-3128.
28. D. Ge, L. Yang, Z. Tong, Y. Ding, W. Xin, J. Zhao and Y. Li, *Electrochim. Acta*, 2013, **104**, 191-197.
29. S. Tian, J. Wang, U. Jonas and W. Knoll, *Chem. Mater.*, 2005, **17**, 5726-5730.
30. L. Y. Yang and W. B. Liau, *Macromol. Chem. Phys.*, 2007, **208**, 994-1001.
31. C. Liu, G. Gao, Y. Zhang, L. Wang, J. Wang and Y. Song, *Macromol. Rapid Comm.*, 2012, **33**, 380-385.
32. L. Santos, P. Martin, J. Ghilane, P. C. Lacaze and J. C. Lacroix, *ACS Appl. Mater. Interfaces*, 2013, **5**, 10159-10164.
33. L. Y. Yang and W. B. Liau, *Synth. Met.*, 2010, **160**, 609-614.
34. D. Wu, F. Xu, B. Sun, R. Fu, H. He and K. Matyjaszewski, *Chem. Rev.*, 2012, **112**, 3959-4015.
35. M. Sharma, G. I. Waterhouse, S. W. C. Loader, S. Garg and D. Svirskis, *Int. J. Pharm.*, 2013, **443**, 163-168.
36. S. W. Choi, Y. Zhang and Y. Xia, *Langmuir*, 2010, **26**, 19001-19006.
37. Y. S. Zhang, S. W. Choi and Y. Xia, *Soft Matter*, 2013, **9**, 9747-9754.
38. A. Power, B. White and A. Morrin, *Electrochim. Acta*, 2013, **104**, 236-241.
39. B. Gorey, J. Galineau, B. White, M. R. Smyth and A. Morrin, *Electroanalysis*, 2012, **24**, 1318-1323.
40. A. M. P. Hussain and A. Kumar, *Bull. Mater. Sci.*, 2003, **26**, 329-334.
41. S. Mu, C. Chen and J. Wang, *Synth. Met.*, 1997, **88**, 249-254.
42. M. M. Gvozdenović, B. Z. Jugović, J. S. Stevanović, T. L. Trišović and B. N. Grgur, *Electropolymerization*, 2011, 77-96.
43. L. Wang, Y. Wan, Y. Li, Z. Cai, H. L. Li, X. S. Zhao and Q. Li, *Langmuir*, 2009, **25**, 6753-6759.
44. E. I. Iwuoha, D. Saenz de Villaverde, N. P. Garcia, M. R. Smyth and J. M. Pingarron, *Biosens. Bioelectron.*, 1997, **12**, 749-761.

[a] *National Centre for Sensor Research, School of Chemical Sciences, Dublin City University, Dublin 9, Ireland. Tel: 00353(1)7006730 E-mail: aoife.morrin@dcu.ie*